Journal of Organometallic Chemistry 762 (2014) 48–57

Contents lists available at ScienceDirect

Journal of Organometallic Chemistry

journal homepage: www.elsevier.com/locate/jorganchem

Hydrazone–diacetyl platinum(II) complexes: Substituent effect on intramolecular N–H···O hydrogen-bond strength

Tim Kluge [a], Eileen Bette [a,b], Martin Bette [a], Jürgen Schmidt [b], Dirk Steinborn [a,*]

[a] Institute of Chemistry–Inorganic Chemistry, Martin Luther University Halle-Wittenberg, Kurt-Mothes-Straße 2, D-06120 Halle, Germany
[b] Department of Bioorganic Chemistry, Leibniz Institute of Plant Biochemistry, Weinberg 3, D-06120 Halle, Germany

ARTICLE INFO

Article history:
Received 10 December 2013
Received in revised form
3 February 2014
Accepted 28 March 2014

Keywords:
Organoplatinum complexes
Acetyl ligands
Hydrazone ligands
Hydrogen-bond strength

ABSTRACT

Bis(benzylamine)diacetylplatinum(II) (**3**) reacted with 2-pyridyl-functionalized hydrazones and with diacetyl dihydrazone to yield diacetyl platinum(II) complexes [Pt(COMe)$_2$(2-pyCR=NNH$_2$)] (R = H, **4a**; Me, **4b**; Ph, **4c**) and [Pt(COMe)$_2$(H$_2$NN=CMe–CMe=NNH$_2$)] (**5**). These complexes showed weak intramolecular N–H···O hydrogen bonds where the hydrazone and the acetyl ligand act as H donor and H acceptor, respectively. Using hydrazones 2-pyCR=NNHR′ substituted with electron-withdrawing groups R′ resulted in complexes [Pt(COMe)$_2$(2-pyCR=NNHR′)] (R/R′ = H/C$_6$H$_4$-*p*-F, **6d**; Me/C$_6$H$_4$-*p*-F, **6e**; H/COMe, **7a**; Me/COMe, **7b**; H/COPh, **7c**; Me/COPh, **7d**; H/CO(C$_6$H$_4$-*p*-F), **7e**; Me/CO(C$_6$H$_4$-*p*-F), **7f**) with stronger intramolecular N–H···O hydrogen bonds. The isolation of the analogous phenylhydrazone complexes (R′ = Ph) failed on this way, but reactions of the 1D coordination polymer [{Pt(COMe)$_2$}$_n$] (**2**) with phenylhydrazones resulted in the formation of the desired complexes [Pt(COMe)$_2$(2-pyCR=NNHR′)] (R/R′ = H/Ph, **6a**; Me/Ph, **6b**; Ph/Ph, **6c**; H/C$_6$F$_5$, **6f**). The constitution of all complexes was unambiguously confirmed analytically, spectroscopically and, in part, by single-crystal X-ray diffraction analyses. Structural and NMR parameters gave evidence that the strength of the N–H···O hydrogen bond is increased in the order **5** ≈ **4a**–**c** < **6a**–**e** < **6f** ≈ **7a**–**f**. This goes parallel with an activation of the acetyl ligand, but in no case the reaction with amines resulted in the formation of iminoacetyl platinum(II) complexes as it was found in analogous oxime–diacetyl complexes [Pt(COMe)$_2$(2-pyCR=NOH)] which have stronger (even than in type **6f**/**7a**–**f** complexes) intramolecular O–H···O hydrogen bonds.

Introduction

In diacetyl platinum(II) complexes bearing 2-pyridyl ket-/aldoxime ligands (**I**) or dioxime ligands (**II**) the oxime ligands act as H donor and the O acetyl atoms as H acceptor, thus forming relatively strong intramolecular O–H···O hydrogen bonds both in the solid state and in solution (Scheme 1) [1]. This gives rise to an activation of the acetyl ligands, and complexes **I** and **II** were found to react with primary amines in a Schiff-base type reaction under formation of iminoacetyl complexes **III** and **IV**, respectively. The characteristic structural features of these complexes are also intramolecular hydrogen bonds in which the iminoacetyl and oxime ligands act as H donor and H acceptor, respectively. Thus, in these complexes protonated iminoacetyl ligands, i.e. aminocarbene ligands, and deprotonated oxime ligands are present [1].

Type **I** and **II** complexes were synthesized from reactions of the dinuclear platina-β-diketone (**1**), an acetyl–hydroxycarbene complex which is stabilized by intramolecular O–H···O hydrogen bonds [2], with 2-pyridyl-functionalized monoximes or with dioximes in the presence of bases such as NaOMe (Scheme 1) [1]. Alternatively, as shown with the reaction of dimethylglyoxime as example, the 1D coordination polymer [{Pt(COMe)$_2$}$_n$] (**2**), in which κC:κ*O* bridging acetyl ligands are present, can be used as precursor complex [3]. Furthermore, in bis(amine)–diacetyl platinum(II) complexes such as **3** the weakly coordinated amine ligands were found to be prone of ligand substitution reactions [4,5]. Due to the amine cleaved off in these reactions, complexes **3** reacted with oximes directly yielding type **III**/**IV** complexes (Scheme 1) [1].

The activation of acetyl ligands for reactions **I** → **III** and **II** → **IV** (Scheme 1) were found to be strongly dependent on the strength of the intramolecular hydrogen bond and on the nucleophilicity of the amine [1]. Structurally related to oximes are hydrazones which can

* Corresponding author. Tel.: +49 345 55 25620; fax: +49 345 55 27028.
E-mail address: dirk.steinborn@chemie.uni-halle.de (D. Steinborn).

http://dx.doi.org/10.1016/j.jorganchem.2014.03.030
0022-328X/

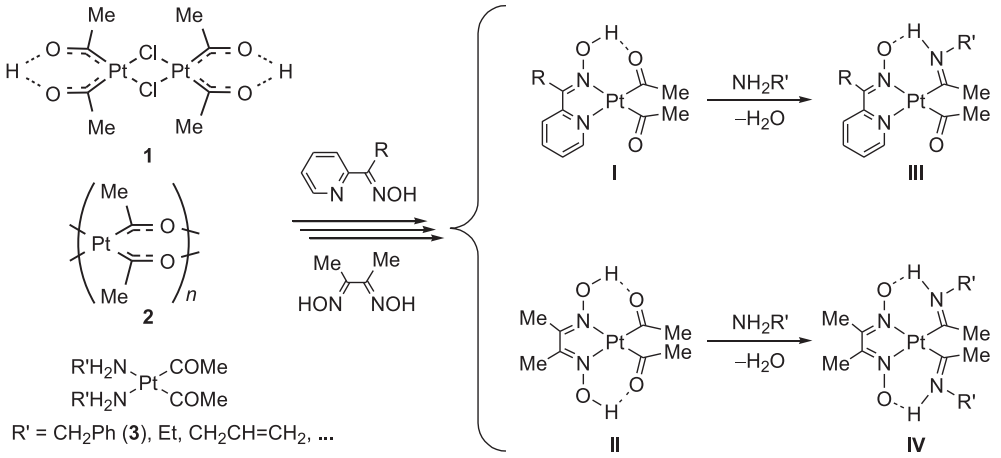

Scheme 1.

also act as H donor in hydrogen bonds. Thus, it is of interest to investigate whether diacetyl platinum(II) complexes with hydrazone co-ligands can be prepared and whether N–H···O hydrogen bonds were formed which are strong enough to activate the acetyl ligands for Schiff-base type reactions.

Results and discussion

Syntheses

Bis(benzylamine)diacetylplatinum(II) (**3**) was found to react with 2-pyridyl-functionalized hydrazones 2-pyCR=NNH$_2$ (R = H, Me, Ph) and with diacetyl dihydrazone under ligand substitution yielding diacetyl platinum(II) complexes bearing the respective hydrazone (**4a**–**c**) and dihydrazone ligand (**5**) (Scheme 2, reaction path **A**). The complexes were isolated in good yields (54–95%) as red (**4a**), orange colored (**4b**/**c**), and yellow (**5**) microcrystals. The constitution of all complexes was unambiguously prooved by high-resolution ESI mass spectrometry, by NMR (^{1}H, ^{13}C, ^{195}Pt) and IR spectroscopy, and by single-crystal X-ray diffraction analyses (**4b**/**c**, **5**).

As for the respective oxime complexes **I** that exhibit intramolecular O–H···O hydrogen bonds (Scheme 1), the hydrazone complexes described here form intramolecular N–H···O hydrogen bonds. To strengthen these hydrogen bonds the terminal N atom of the hydrazone was substituted by electron-withdrawing groups (R′). Thus, phenylhydrazones 2-pyCR=NNHR′ (R′ = Ph, C$_6$H$_4$-*p*-F, C$_6$F$_5$) and acyl substituted hydrazones 2-pyCR=NNH(COR″) (R″ = Me, Ph, C$_6$H$_4$-*p*-F), i.e. acid hydrazides, were reacted with bis(benzylamine)diacetylplatinum(II) (**3**) (Scheme 2, **B**/**C**). In all cases the reaction mixtures became immediately red and diacetyl platinum(II) complexes bearing fluorophenyl (**6d**/**e**) and acyl

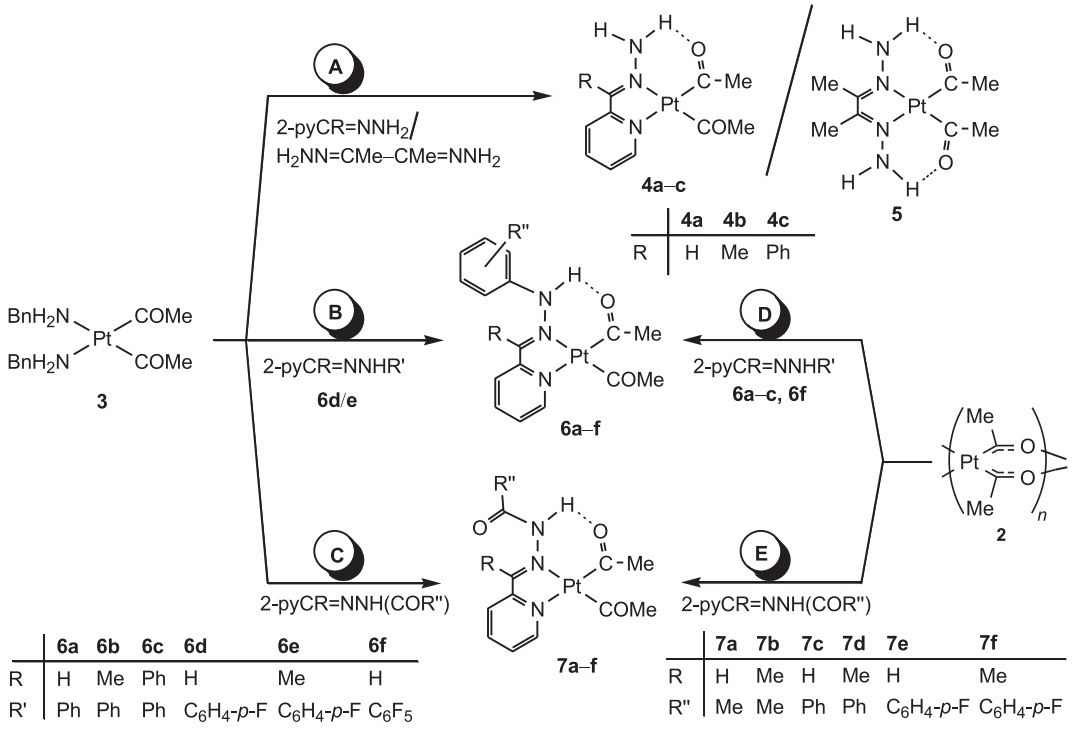

	4a	4b	4c
R	H	Me	Ph

	6a	6b	6c	6d	6e	6f
R	H	Me	Ph	H	Me	H
R'	Ph	Ph	Ph	C$_6$H$_4$-*p*-F	C$_6$H$_4$-*p*-F	C$_6$F$_5$

	7a	7b	7c	7d	7e	7f
R	H	Me	H	Me	H	Me
R"	Me	Me	Ph	Ph	C$_6$H$_4$-*p*-F	C$_6$H$_4$-*p*-F

Scheme 2.

substituted (**7a**–**f**) 2-pyridyl-functionalized hydrazone ligands could be isolated in good yields (65–83%). In the case of the phenyl and pentafluorophenyl substituted hydrazones 2-pyCR=NNHPh and 2-pyCR=NNH(C_6F_5), respectively, the reaction mixtures became also immediately red, thus indicating the formation of complexes **6a**–**c** and **6f**, but their isolation failed. Instead, only the starting complex **3** could be re-formed. To obtain these complexes, the 1D coordination polymeric diacetyl bridged platinum(II) complex **2** was reacted with 2-pyCR=NNHR′ (R′ = Ph, C_6F_5, Scheme 2, **D**). On this way **6a**–**c** and **6f** could be isolated in a pure state in 71–83% yields. Using this method for the synthesis of complexes **6d**/**e**, the isolated products contained unidentified side products, whereas complexes **7a**–**f** were obtained in a pure state (Scheme 2, **E**). All complexes were fully characterized by microanalyses or high-resolution ESI mass spectrometry, by NMR (^{1}H, ^{13}C, (^{19}F), ^{195}Pt) and IR spectroscopy, as well as by single-crystal X-ray diffraction analyses (**6a**, **7a**, **7c**·CH_2Cl_2, **7e**).

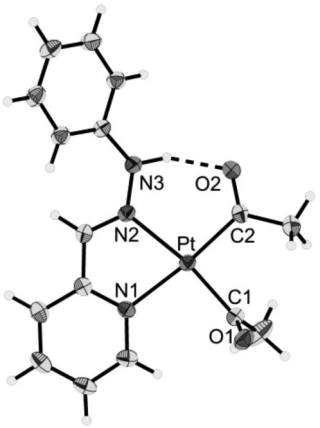

Fig. 2. Molecular structure of [Pt(COMe)$_2$(2-pyCH=NNHPh)] (**6a**, displacement ellipsoids of non-hydrogen atoms at 30% probability). The broken line indicates an intramolecular N–H···O hydrogen bond.

Structural characterization

From single-crystal X-ray diffraction analyses of [Pt(COMe)$_2$(2-pyCR=NNHR′)] (R/R′ = Me/H, **4b**; Ph/H, **4c**; H/Ph, **6a**; H/COMe, **7a**; H/COPh, **7c**·CH_2Cl_2; H/CO(C_6H_4-*p*-F), **7e**) molecular structures of the complexes were obtained. They are shown in Figs. 1–3; selected structural parameters are given in Table 1. The asymmetric units of crystals of complexes **4c** and **7a** contain two symmetry-independent molecules with very similar structures. In all complexes the platinum atoms are coordinated in a square-planar fashion (sum of angles between neighbored ligands: 360.0–360.3°) by two acetyl ligands and a κ^2*N*,*N*′ coordinated pyridyl-functionalized hydrazone ligand. Due to this bidentate coordination the N1–Pt–N2 angles are considerably smaller (75.6(2)–76.5(8)°) than 90°. Notably, these angles are even smaller than those in platinum(II) complexes with bidentately coordinated 2-pyCR=NR′ (R/R′ = H, alkyl, aryl) ligands (median 79.8°; lower/upper quartile 78.5/80.1°; *n* = 29, *n* = number of observations [6]).

In all these complexes the N–H group and an O atom of an acetyl ligand act as H donor and H acceptor, respectively, thus forming intramolecular N–H···O hydrogen bonds (graph set [7]: *S*(6)). The N···O distances (2.653(7)–2.855(6) Å) and the N–H···O angles (141–159°) indicate moderately strong hydrogen bonds [8]. On the basis of the distance criterion it will be obvious that a substitution at the terminal N atom of the hydrazone ligand with electron-withdrawing groups R′ gives rise to stronger hydrogen bonds: R′ = H (2.740(7)–2.855(6) Å, **4b**/**c**) < R′ = Ph (2.701(3) Å, **6a**) < R′ = COR″ (2.653(7)–2.684(4) Å, **7a**/**c**/**e**). Additionally, in type **7** complexes the O3 atoms of the acyl substituents act as H acceptor in weak intramolecular C3–H···O3 hydrogen bonds (C3···O3 2.758(5)–2.809(5) Å, C3–H···O3 118–123°).

Except for complex **4b**, due to the intramolecular N–H···O hydrogen bonds the acetyl ligands which are involved in these hydrogen bonds lie nearly in the complex planes (3.8(5)–29.6(4)°) whereas the other ones, as usual [3,5,9], are nearly perpendicularly arranged (72.1(5)–85.1(4)°). In complex **4b** the two acetyl ligands form angles with the complex plane of 46.0(2) and 48.7(1)°. This might be reasoned by weak intermolecular N3–H···O1′ hydrogen bonds (Fig. 1; N3···O1′ 3.019(5) Å, N3–H···O1′ 155°, graph set [7]: C(6)) which give rise to a 1D network of hydrogen bonds in crystals of **4b**. Analogously, intermolecular hydrogen bonds link the two symmetry-independent molecules in complex **4c** (N3···O4/N6···O2 2.986(8)/2.812(9) Å, N3–H···O4/N6–H···O2 124/112°, graph set: $R_2^2(12)$, Fig. 1) so that dinuclear entities are formed in crystals of **4c**.

The molecular structure of the diacetyl platinum complex **5** bearing a dihydrazone ligand is shown in Fig. 4 and structural

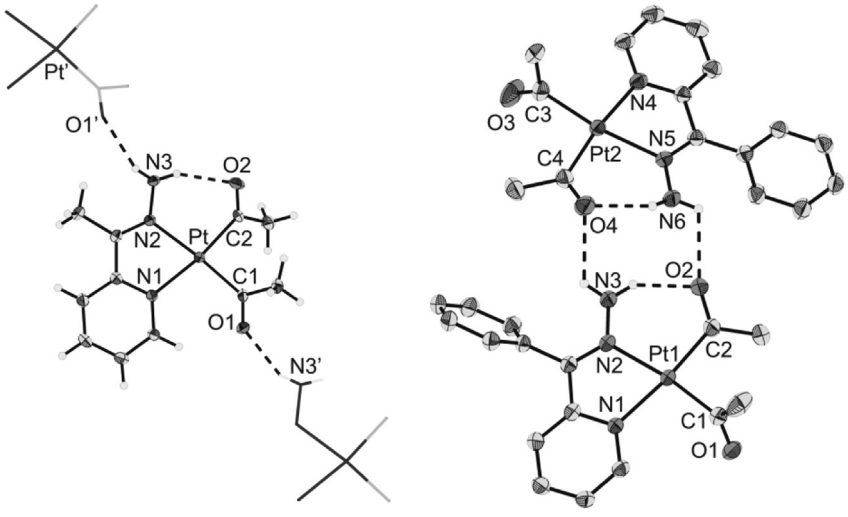

Fig. 1. Structures of [Pt(COMe)$_2$(2-pyCR=NNH$_2$)] in crystals of **4b** (R = Me, left) and **4c** (R = Ph, right; all displacement ellipsoids of non-hydrogen atoms at 30% probability, on the right H atoms are not shown except hydrogen bonded ones). The broken lines indicate intra- and intermolecular N–H···O hydrogen bonds.

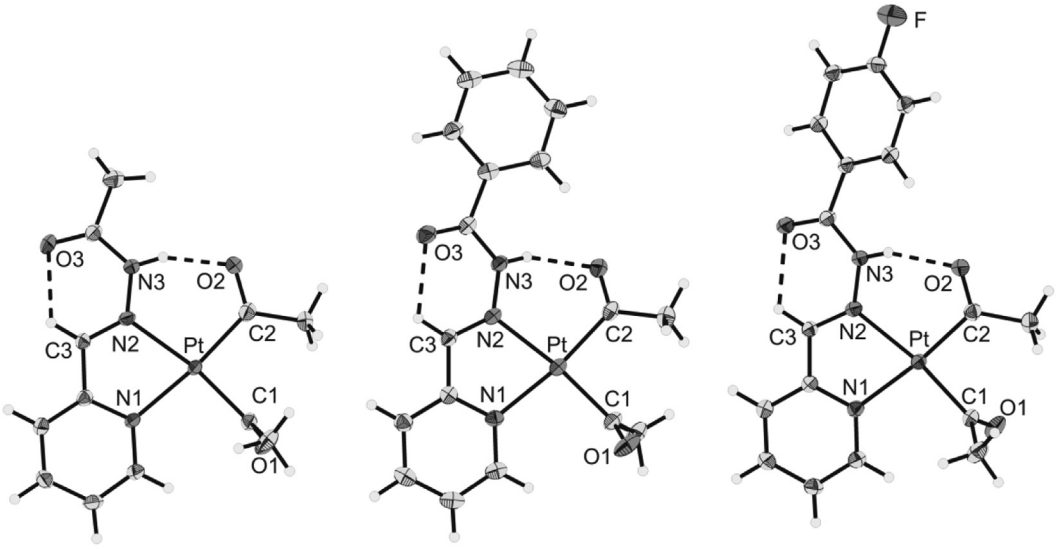

Fig. 3. Structures of [Pt(COMe)$_2$(2-pyCH=NNHR′)] in crystals of **7a** (R′ = COMe, left; one of the two symmetry-independent molecules is shown), **7c**·CH_2Cl_2 (R′ = COMe, middle), and **7e** (R′ = CO(C_6H_4-*p*-F), right; all displacement ellipsoids of non-hydrogen atoms at 30% probability). The broken lines indicate intramolecular N–H···O and C–H···O hydrogen bonds.

parameters are given in the Figure caption. The platinum atom is square-planar coordinated (sum of angles: 360.0°) by two acetyl ligands and the bidentately κ^2N,N' coordinated dihydrazone ligand. The dihydrazone ligand gives rise to the formation of two intramolecular N–H···O hydrogen bonds. As for the complexes with 2-pyCR=NNHR′ ligands, the N···O distances (N4···O1/N3···O2 2.800(5)/2.982(5) Å) and the N–H···O angles (N4–H···O1/N3–H···O2 146/148°) give evidence for moderately strong hydrogen bonds [8]. The two acetyl ligands are twisted out of the complex plane by 30.5(2)° and 50.7(3)°, respectively, whereas the smaller interplanar angle belongs to the shorter N···O distance and hence stronger hydrogen bond (N4–H···O1).

The large difference of 0.182 Å between the two N···O distances can be traced back to intermolecular hydrogen bonds found in crystals of **5** (Fig. 5). On the one side, intermolecular N3–H···N4′ hydrogen bonds (N3···N4′ 3.126(5) Å, N3–H···N4′ 144°) are formed (graph set [7]: C(6)). On the other side, non-conventional N4–H···Pt′ hydrogen bonds, in which the doubly occupied $6d_{z2}$ orbital of Pt acts as H acceptor [10], are formed (graph set [7]: *C*(4)) such that the crystal is threaded by a 2D network of hydrogen bonds. Altogether, the $N4H_2$ group acts both as H donor and as H acceptor whereas the $N3H_2$ group functions only as H donor. According to the concept of the σ-bond cooperativity [8], this could be the reason for the stronger intramolecular N4–H···O1 bond compared with the N3–H···O2 one. In accordance with this, DFT calculations (details see Supplemental material) of complex **5**, representing the structure of an isolated molecule in the gas phase, gave proof of a nearly C_2 symmetric molecule having two hydrogen bonds of the same strength (N···O 2.796/2.796 Å, N–H···O 153/153°), see Fig. S1.

Spectroscopic characterization

NMR spectroscopic data proved to be fully consistent with the constitution of the complexes given in Scheme 2. Characteristic ^{1}H,

Table 1
Selected distances (in Å) and angles (in °) of complexes [Pt(COMe)$_2$(2-pyCR=NNHR′)] (**4b**/**c**, **6a**, **7a**, **7c**·CH_2Cl_2, **7e**).

	4b	**4c**[a]	**6a**	**7a**[a]	**7c**·CH_2Cl_2	**7e**
R/R′	Me/H	Ph/H	H/Ph	H/COMe	H/COPh	H/CO(C_6H_4-*p*-F)
Pt–C1	1.988(5)	1.973(5)/1.985(5)	1.985(3)	1.978(7)/1.976(6)	1.982(4)	1.978(4)
Pt–C2	2.004(5)	1.976(6)/1.983(6)	1.994(3)	1.979(7)/1.982(7)	1.984(5)	1.980(4)
Pt–N1	2.126(4)	2.116(4)/2.111(5)	2.119(2)	2.133(5)/2.130(5)	2.130(4)	2.122(4)
Pt–N2	2.132(4)	2.139(4)/2.152(4)	2.160(2)	2.169(5)/2.167(5)	2.144(3)	2.169(3)
C1=O1	1.228(6)	1.217(6)/1.210(7)	1.208(4)	1.230(9)/1.234(9)	1.218(5)	1.222(5)
C2=O2	1.220(6)	1.243(7)/1.232(7)	1.234(3)	1.245(8)/1.258(8)	1.234(5)	1.246(5)
N2–N3	1.370(5)	1.357(6)/1.342(6)	1.347(3)	1.374(8)/1.367(7)	1.372(4)	1.363(5)
C1–Pt–C2	89.7(2)	90.5(2)/90.6(3)	91.3(1)	91.6(3)/91.4(3)	91.0(2)	90.9(2)
C2–Pt–N2	96.3(2)	97.6(2)/97.4(2)	97.7(1)	97.5(2)/97.7(2)	96.1(2)	98.0(2)
N1–Pt–N2	75.6(2)	76.0(2)/75.7(2)	76.5(8)	76.3(2)/76.2(2)	75.9(1)	75.9(1)
N1–Pt–C1	98.7(2)	95.9(2)/96.4(2)	94.5(1)	94.6(2)/94.8(2)	97.0(2)	95.2(2)
γ(c.p./MeC1=O1)[b]	48.7(1)	72.1(5)/72.1(5)	83.0(2)	85.1(4)/85.1(4)	73.9(2)	82.4(6)
γ(c.p./MeC2=O2)[b]	46.0(2)	29.6(4)/29.6(4)	12.5(1)	3.8(5)/3.8(5)	28.4(3)	19.3(6)
N3···O2	2.855(6)	2.790(6)/2.740(7)	2.701(3)	2.669(8)/2.653(7)	2.668(5)	2.684(4)
N3–H···O2[c]	151	147/141	156	155/159	158	154
C3···O3				2.784(8)/2.786(8)	2.809(5)	2.758(5)
C3–H···O3[d]				123/119	118	118

[a] The values of the two symmetry-independent molecules are given separated by a slash.
[b] c.p. = coordination plane.
[c] H atoms found in the electron density maps.
[d] H atoms placed on calculated positions.

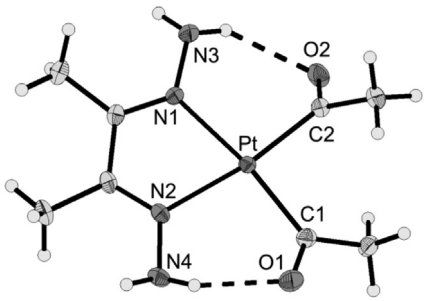

Fig. 4. Molecular structure of $[Pt(COMe)_2(NH_2N{=}CMe{-}CMe{=}NNH_2)]$ (**5**, displacement ellipsoids of non-hydrogen atoms at 30% probability). The broken lines indicate intramolecular N–H···O hydrogen bonds. Selected distances (in Å) and angles (in °): Pt–C1 1.999(4), Pt–C2 1.993(4), Pt–N1 2.131(3), Pt–N2 2.128(3), C1–O1 1.226(5), C2–O2 1.221(5), N1–N3 1.365(4), N2–N4 1.377(4), C1–Pt–N2 97.6(1), C1–Pt–C2 91.5(2), C2–Pt–N1 96.1(1), N1–Pt–N2 74.8(1), γ(c.p./MeC1=O1) 30.5(2), γ(c.p./MeC2=O2) 50.7(3) (c.p. = coordination plane), N3···O2 2.982(5), N4···O1 2.800(5), N3–H···O2 148, N4–H···O1 146.

^{13}C, and ^{195}Pt NMR spectroscopic parameters of complexes **4**–**7** are compiled in Table 2. Due to the different ligands in *trans* position (except for complex **5**), two sets of signals with typical platinum coupling constants were found for the two acetyl ligands. HSQC measurements allowed to assign the methyl protons of the acetyl ligands to the corresponding C atoms. With complex **7e** as example, the respective carbonyl C atom was identified via HMBC measurements. Furthermore, a NOESY experiment (coupling between $COCH_3$ at 2.59 ppm and H^6(py) at 8.52 ppm) exhibited which acetyl ligand is *trans* to the hydrazone N atom and which one *trans* to the pyridine N atom. On this basis the acetyl ligands of the other complexes were assigned (Table 2). This assignment is consistent with that of the pyridyl-functionalized oxime complexes (type **I**, Scheme 1) [1]. The platinum chemical shifts were found in the expected range (−3364 to −3444 ppm) and did not show a characteristic dependence on the substitution pattern of the hydrazone ligand [1,3,5].

In an N–H···O hydrogen bond the N*H* shift can be regarded as a measure for the hydrogen-bond strength [8]. On this basis, the following dependence of the N–H···O hydrogen-bond strength on the substitution pattern of the hydrazone group =NNHR′ was found: R′ = acyl (12.40–14.35 ppm; **7a**–**f**) ≈ C_6F_5 (12.43 ppm; **6f**) > Ph, C_6H_4-*p*-F (9.97–11.63 ppm; **6a**–**e**) > H (6.61–8.08 ppm; **4a**–**c**/**5**). Furthermore, as shown by low-field shifts of the N*H* signals by 0.4–1.7 ppm in complexes bearing 2-pyCH=NNHR′ ligands compared to those bearing 2-pyCR=NNHR′ (R = Me, Ph) ligands, the former ones tend to form stronger N–H···O hydrogen bonds. At room temperature (**4a**–**c**/**5**) and at −85 °C (**4b**), for the complexes bearing non-substituted hydrazone ligands, only one signal for the two NH_2 protons were found. Furthermore, for all complexes, except for complexes **4**, characteristic $^3J_{Pt,H}$ coupling constants of 15–20 Hz were observed.

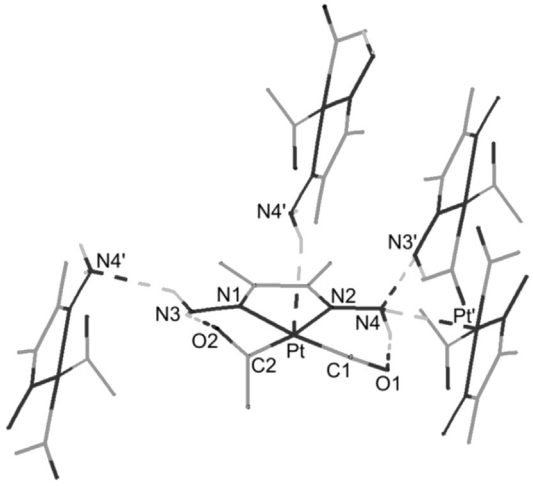

Fig. 5. Wire model of $[Pt(COMe)_2(H_2NN{=}CMe{-}CMe{=}NNH_2)]$ in crystals of **5** showing the inter- and intramolecular hydrogen bonds (broken lines). Hydrogen atoms are omitted for clarity, except those which are involved in hydrogen bonds. Selected distances (in Å) and angles (in °): N3···O2 2.982(5), N3–H···O2 148, N4···O1 2.800(5), N4–H···O1 146, N3···N4′ 3.126(5), N3–H···N4′ 144, N4···Pt′ 3.413(4), N4–H···Pt′ 135.

The stronger the intramolecular N–H···O hydrogen bond the more the acetyl ligand involved in this hydrogen bond is activated for a nucleophilic attack. When type **I** oxime–diacetyl platinum(II) complexes are obtained analogously as the hydrazone–diacetyl complexes described here (Scheme 2, **A**–**C**), the O–H···O hydrogen bonds formed were strong enough to activate the acetyl ligands such that with the benzylamine cleaved off type **III** iminoacetyl platinum(II) complexes were obtained in a Schiff-base type reaction, cf. Scheme 1 [1]. Here, in no case, not even in type **6f**/**7a**–**f** complexes with the strongest N–H···O hydrogen bonds, a formation of iminoacetyl platinum(II) complexes was observed. Therefore, complexes **4a**–**c**, **6d**/**f**, and **7c** were reacted with a 10- and 100-fold excess of benzylamine ($pK_a = 9.3$; here and in the following the pK_a values of the corresponding RNH_3^+ cations are given [11]) and complex **7e** with 5-fold excess of the more basic 2-phenylethylamine (pK_a = 9.8) and ethylamine (pK_a = 10.6), but NMR spectra of reaction solutions or isolated solids indicated in no case the formation of iminoacetyl complexes. Even in the presence of a water scavenger (molecular sieve 4A) an iminoacetyl complex formation did not take place.

Conclusions

The investigations presented in this work exhibited that in diacetyl platinum(II) complexes bearing 2-pyridyl-functionalized hydrazone (**4**, **6**, **7**) and dihydrazone (**5**) ligands intramolecular N–H···O hydrogen bonds are present both in the solid state and in solution. The chemical shifts of the hydrogen bonded protons δ(N*H*) and the N···O distances can be regarded as a measure of the hydrogen-bond strength [8]. As expected, it increases with increasing electron-withdrawing character of the substituents R′ at the terminal N atoms (Fig. 6). But in all cases, these hydrogen bonds were proven to be weaker than the O–H···O hydrogen bonds in the respective oxime complexes. As experimentally shown here, the expected activation of the acetyl ligands by the hydrogen bonds – in contrast to that in oxime complexes [1] – is not strong enough to form iminoacetyl complexes with amines in Schiff-base type reactions. In line with all experimental results, DFT calculations show an N–H···O connectivity of intramolecular hydrogen bonds (see global minima in Fig. 7). Relaxed potential energy surface scans with N···H distances as scan coordinate result with fixed N···O distances (to avoid break of the hydrogen bonds, cf. Supplemental Material) in typical double-well potentials of hydrogen bonds (Fig. 7). The transfer from the energetically favored into the unfavored well (N–H···O → N···H–O) costs for **4b***/**7b*** (starred numbers indicate calculated complexes) 15.9/15.9 kcal/mol. The energy demand for the proton transfer within an O–H···O hydrogen bond of an analogous oxime complex (cf. **I*** in Fig. 7) is much smaller (6.9 kcal/mol). Because this proton transfer is the crucial step for the activation of the acetyl ligands, in full accord with the experimental results, oxime–diacetyl platinum(II) complexes are prone to Schiff-base type reactions but not the respective hydrazone complexes.

Table 2
Selected NMR spectroscopic parameters (δ in ppm, J in Hz, in $CDCl_3$) of complexes [Pt(COMe)$_2$(2-pyCR=NNHR′)] (**4a–c**, **6a–f**, **7a–f**)[a] and [Pt(COMe)$_2$(H_2NN=CMe–CMe=NNH_2)] (**5**).

	R/R′	δ_H ($^3J_{Pt,H}$) N*H*	δ_H ($^3J_{Pt,H}$) COC*H*$_3$	δ_C ($^2J_{Pt,C}$) COCH$_3$	δ_C ($^1J_{Pt,C}$) COCH$_3$	δ_{Pt} *Pt*
4a	H/H	8.08	2.25 (28.6)/2.47 (22.1)	43.0 (381)/45.0 (349)	230.8/227.0	−3384
4b	Me/H	7.53	2.21 (28.9)/2.42 (23.4)	43.2 (374)/45.1 (348)	231.6 (1292)/228.7 (1292)	−3397
4c	Ph/H	7.67	2.26 (29.4)/2.47 (24.4)	43.1 (375)/45.0 (355)	230.2 (1298)/228.9 (1295)	−3389
5	–	6.61 (22)	2.30 (26.4)	44.2 (361)	232.1	−3444
6a	H/Ph	11.63 (18)	2.27 (31.2)/2.52 (23.8)	42.7 (375)/44.9 (347)	229.0/228.7	−3395
6b	Me/Ph	10.65 (16)	2.15 (29.7)/2.45 (23.3)	42.9 (371)/45.0 (342)	232.5/228.3	−3404
6c	Ph/Ph	9.97 (19)	2.00 (27.9)/2.39 (23.5)	42.8 (367)/44.4 (361)	229.7/228.7	−3364
6d	H/C_6H_4-*p*-F	11.37 (18)	2.08 (33.5)/2.34 (23.7)	42.7 (370)/44.9 (347)	229.1/228.7	−3397
6e	Me/C_6H_4-*p*-F	10.60 (17)	2.14 (29.6)/2.44 (23.3)	42.8 (375)/45.0 (347)	232.3/228.3	−3408
6f	H/C_6F_5	12.43 (18)	2.27 (32.8)/2.55 (23.3)	42.3 (371)/44.7 (345)	227.9/227.7	−3415
7a	H/COMe	13.50 (18)	2.26 (32.5)/2.52 (23.4)	42.5 (374)/44.7 (340)	228.5/227.9	−3411
7b	Me/COMe	12.40 (15)	2.23 (30.5)/2.45 (23.1)	42.7 (370)/44.0 (339)	230.4/228.7	−3392
7c	H/COPh	14.25 (18)	2.28 (32.4)/2.54 (23.5)	42.4 (370)/44.7 (346)	229.1/227.7	−3413
7d	Me/COPh	13.34 (17)	2.21 (30.9)/2.48 (22.9)	42.6 (370)/44.9 (340)	230.4/229.0	−3396
7e	H/CO(C_6H_4-*p*-F)	14.35 (20)	2.33 (32.8)/2.59 (23.4)	42.4 (374)/44.7 (347)	229.4/227.8	−3412
7f	Me/CO(C_6H_4-*p*-F)	13.40 (16)	2.20 (31.5)/2.48 (28.5)	42.7 (372)/44.9 (335)	230.4/229.2	−3395

[a] The NMR parameters of the acetyl ligands *trans* to the N_{py} and the $N_{hydrazone}$ atoms are given separated by a slash.

Experimental section

General comments

All reactions were performed in an argon atmosphere using the standard Schlenk techniques. Solvents were dried (diethyl ether and *n*-pentane over Na/benzophenone; $CHCl_3/CH_2Cl_2$ over CaH_2) and distilled prior to use. NMR spectra were recorded at 27 °C with Varian Gemini 200, VXR 400, and Unity 500 spectrometers. Chemical shifts are relative to the solvent signals of $CDCl_3$ (δ_H 7.24, δ_C 77.0) as internal references; $\delta(^{195}Pt)$ is referenced to $Na_2[PtCl_6]$; $\delta(^{19}F)$ is relative to external CCl_3F. If necessary, 2D NMR techniques (COSY, HSQC, HMBC and NOESY) were used to assign the signals in ^1H and ^{13}C NMR spectra. IR spectra were recorded by a Bruker Tensor 28 spectrometer with a Platinum ATR unit. Microanalyses were performed by the University of Halle microanalytical laboratory using Vario EL (Elementar Analysensysteme) elemental analyzer. The high-resolution ESI mass spectra were obtained from a Bruker Apex III Fourier transform ion cyclotron resonance (FT-ICR) mass spectrometer (Bruker Daltonics) equipped with an infinity cell, a 7.0 T superconducting magnet (Bruker), an rf-only hexapole ion guide, and an external APOLLO electrospray ion source (Agilent, off-axis spray). The sample solutions were introduced continuously via a syringe pump with a flow rate of 120 μL h^{-1}. The platinum(II) precursor complexes [{Pt(COMe)$_2$}$_n$] (**2**) [3] and [Pt(COMe)$_2$(NH_2Bn)$_2$] (**3**) [4] as well as the hydrazones/dihydrazones [12–15] (NMR data cf. Supplemental material) were prepared according to literature methods.

*Syntheses of complexes **4** and **5** with hydrazone ligands of the type 2-pyCR=NNH_2 and H_2NN=CMe–CMe=NNH_2*

At room temperature, [Pt(COMe)$_2$(NH_2Bn)$_2$] (**3**) (80 mg, 0.16 mmol) and 2-pyCR=NNH_2 (R = H, Me, Ph; 0.16 mmol) or H_2NN=CMe–CMe=NNH_2 (0.16 mmol) were dissolved in methylene chloride (5 mL) and the reaction mixture was stirred for one hour. The volume of the resulting orange colored (**4**) or dark yellow (**5**) solution was reduced to ca. 1 mL in vacuo. After the addition of diethyl ether (1 mL) and *n*-pentane (2 mL) a precipitate was obtained, which was filtered off, washed with diethyl ether (3 × 5 mL), and dried in vacuo.

[Pt(COMe)$_2$(2-pyCH=NNH_2)] (**4a**). Yield: 35 mg (54%). HRMS (ESI): *m/z* calcd for $[C_{10}H_{13}N_3O_2PtNa]^+$ 425.05477, found for $[M + Na]^+$ 425.05506. ^1H NMR ($CDCl_3$, 500 MHz): δ 2.25 (s + d, $^3J_{Pt,H}$ = 28.6 Hz, 3H, COC*H*$_3$), 2.47 (s + d, $^3J_{Pt,H}$ = 22.1 Hz, 3H, COC*H*$_3$), 7.26 (m, 1H, *H*^{5} py), 7.39 (m, 1H, *H*^{3} py), 7.83 (m, 1H, *H*^{4} py), 8.08 (s, 2H, N*H*$_2$), 8.20 (s, 1H, C*H*=NNH_2), 8.28 (m, 1H, *H*^{6} py). ^{13}C NMR ($CDCl_3$, 125 MHz): δ 43.0 (s + d, $^2J_{Pt,C}$ = 381 Hz, $COCH_3$), 45.0 (s + d,

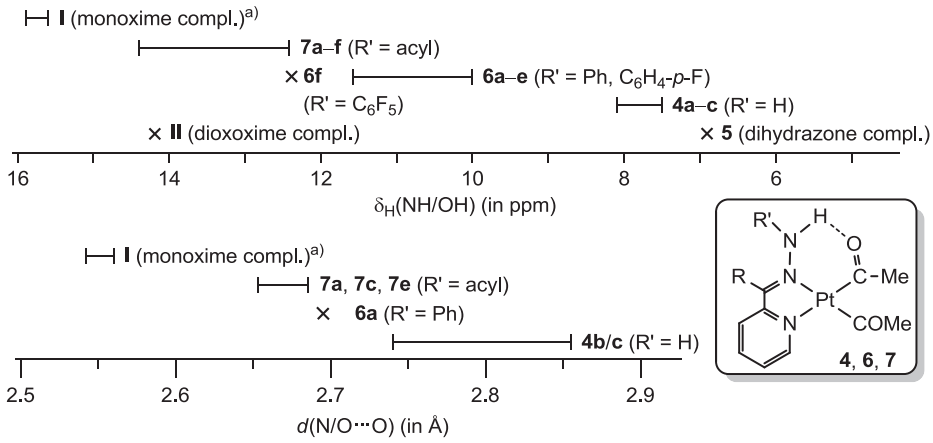

Fig. 6. Chemical shifts of the hydrogen-bonded protons (top) and N···O distances (bottom) as parameters for the strength of the intramolecular N–H···O hydrogen bonds in hydrazone–diacetyl platinum(II) complexes. For comparison, the corresponding values of O–H···O hydrogen bonds in oxime–diacetyl platinum(II) complexes of types **I** and **II** (cf. Scheme 1) are given [1]. a) 3 entries.

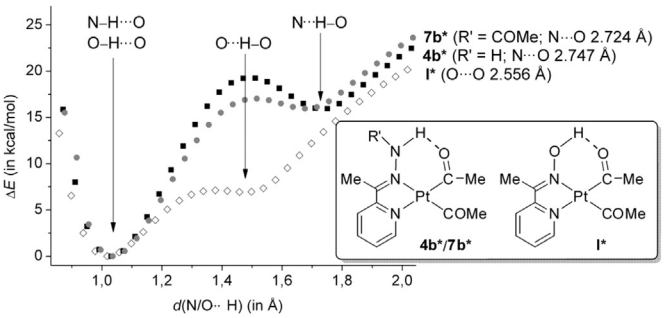

Fig. 7. Relaxed potential energy surface scans with N···H distances as scan coordinate with fixed N···O distances of hydrazone–diacetyl platinum(II) complexes **4b*** (■) and **7b*** (●). Additionally, the structures representing the global minima were characterized as equilibrium structures which is not the case for the local minima (see Supplemental material). The oxime–diacetyl platinum(II) complex **I*** (◇, see formula sketch and Ref. [1]) is given for comparison (O···H distance as scan coordinate with fixed O···O distance).

$^2J_{Pt,C}$ = 349 Hz, COCH$_3$), 122.9 (s, C^3 py), 124.3 (s, C^5 py), 138.7 (s, CH=NNH$_2$), 139.2 (s, C^4 py), 150.3 (s + d, $^2J_{Pt,C}$ = 47 Hz, C^6 py), 155.4 (s, C^2 py), 227.0 (s, COCH$_3$), 230.8 (s, COCH$_3$). ^{195}Pt NMR (CDCl$_3$, 107 MHz): δ −3384 (s). IR 3257(w), 3130(w), 1610(m), 1545(m) cm^{-1}.

[Pt(COMe)$_2$(2-pyCMe=NNH$_2$)] (**4b**). Yield: 57 mg (84%). HRMS (ESI): *m/z* calcd for [C$_{11}$H$_{15}$N$_3$O$_2$PtNa]$^+$ 439.07042, found for [M + Na]$^+$ 439.07039. ^{1}H NMR (CDCl$_3$, 200 MHz): δ 2.21 (s + d, $^3J_{Pt,H}$ = 28.9 Hz, 6H, COCH$_3$ + C(CH$_3$)=NNH$_2$), 2.42 (s + d, $^3J_{Pt,H}$ = 23.4 Hz, 3H, COCH$_3$), 7.31 (m, 1H, H^5 py), 7.53 (m, 3H, H^3 py + NH$_2$), 7.90 (m, 1H, H^4 py), 8.37 (m, 1H, H^6 py). ^{13}C NMR (CDCl$_3$, 50 MHz): δ 12.6 (s, C(CH$_3$)=NNH$_2$), 43.2 (s + d, $^2J_{Pt,C}$ = 373.7 Hz, COCH$_3$), 45.1 (s + d, $^2J_{Pt,C}$ = 347.8 Hz, COCH$_3$), 121.9 (s, C^3 py), 124.7 (s + d, $^3J_{Pt,C}$ = 20 Hz, C^5 py), 139.0 (s, C^4 py), 146.5 (s, C(CH$_3$)=NNH$_2$), 150.4 (s + d, $^2J_{Pt,C}$ = 44 Hz, C^6 py), 156.1 (s, C^2 py), 228.7 (s + d, $^1J_{Pt,C}$ = 1292 Hz, COCH$_3$), 231.6 (s + d, $^1J_{Pt,C}$ = 1292 Hz, COCH$_3$). ^{195}Pt NMR (CDCl$_3$, 107 MHz): δ −3397 (s). IR 3294(m), 3151(m), 1583(m), 1564 (m) cm^{-1}.

[Pt(COMe)$_2$(2-pyCPh=NNH$_2$)] (**4c**). Yield: 62 mg (80%). HRMS (ESI): *m/z* calcd for [C$_{16}$H$_{17}$N$_3$O$_2$PtNa]$^+$ 501.08607, found for [M + Na]$^+$ 501.08649. ^{1}H NMR (CDCl$_3$, 200 MHz): δ 2.26 (s + d, $^3J_{Pt,H}$ = 29.4 Hz, 3H, COCH$_3$), 2.47 (s + d, $^3J_{Pt,H}$ = 24.4 Hz, 3H, COCH$_3$), 6.93 (m, 1H, H^3 py), 7.23–7.37 (m, 3H, H^5 py + H Ph), 7.54–7.64 (m, 3H, H Ph), 7.67 (s, 2H, NH$_2$), 7.74 (m, 1H, H^4 py), 8.52 (m, 1H, H^6 py). ^{13}C NMR (CDCl$_3$, 50 MHz): δ 43.1 (s + d, $^2J_{Pt,C}$ = 375.4 Hz, COCH$_3$), 45.0 (s + d, $^2J_{Pt,C}$ = 355.3 Hz, COCH$_3$), 123.2 (s, C^3 py), 124.4 (s + d, $^3J_{Pt,C}$ = 19 Hz, C^5 py), 128.4 (s, *o-C*/*m-C* Ph), 129.1 (s, *i-C*), 130.3 (s, *o-C*/*m-C* Ph), 130.8 (s, *p-C* Ph), 138.8 (s, C^4 py), 146.8 (s, CPh=NNH$_2$), 150.6 (s + d, $^2J_{Pt,C}$ = 45 Hz, C^6 py), 156.6 (s, C^2 py), 228.9 (s + d, $^1J_{Pt,C}$ = 1295 Hz, COCH$_3$), 230.2 (s + d, $^1J_{Pt,C}$ = 1298 Hz, COCH$_3$). ^{195}Pt NMR (CDCl$_3$, 86 MHz): δ −3389 (s). IR 3371(m), 3115(m), 1612(m), 1562(m) cm^{-1}.

[Pt(COMe)$_2$(H$_2$NN=CMe–CMe=NNH$_2$)] (**5**). Yield: 61 mg (95%). HRMS (ESI): *m/z* calcd for [C$_8$H$_{16}$N$_4$O$_2$PtNa]$^+$ 418.08132, found for [M + Na]$^+$ 418.08177. ^{1}H NMR (CDCl$_3$, 200 MHz): δ 2.01 (s, 6H, H$_2$NN=CCH$_3$), 2.30 (s + d, $^3J_{Pt,H}$ = 26.4 Hz, 6H, COCH$_3$), 6.61 (s + d, $^3J_{Pt,H}$ = 21.5 Hz, 4H, NH$_2$). ^{13}C NMR (CDCl$_3$, 125 MHz): δ 13.8 (s, H$_2$NN=CCH$_3$), 44.2 (s + d, $^2J_{Pt,C}$ = 361.1 Hz, COCH$_3$), 150.3 (s, H$_2$NN=CCH$_3$), 232.1 (s, COCH$_3$). ^{195}Pt NMR (CDCl$_3$, 86 MHz): δ −3444 (s). IR 3346(m), 3234(m), 3198(w), 3107(m), 1549 (m) cm^{-1}.

*Syntheses of complexes **6a–c** and **6f** with phenylhydrazone ligands*

At −78 °C, to a suspension of [{Pt(COMe)$_2$}$_n$] (**2**) (40 mg, 0.14 mmol) in methylene chloride (15 mL) an equimolar amount of 2-pyCR=NNHPh (R = H, Me, Ph; 0.14 mmol) or an excess of 20% of 2-pyCH=NNH(C$_6$F$_5$) (49 mg, 0.17 mmol) was added dropwise. After stirring for 30 min at this temperature, the orange colored reaction mixture was warmed up to room temperature and stirred for further 8 h. The solvent of the red solution was reduced to ca. 1 mL and diethyl ether (3 mL) was added. The red (**6a–c**) and orange colored (**6f**) precipitate obtained was filtered off, washed with diethyl ether (3 × 3 mL), and dried in vacuo.

[Pt(COMe)$_2$(2-pyCH=NNHPh)] (**6a**). Yield: 53 mg (78%). Anal. found (calc.): C$_{16}$H$_{17}$N$_3$O$_2$Pt (478.41 g/mol), C 39.91 (40.17), H 3.36 (3.58), N 8.84 (8.78). ^{1}H NMR (CDCl$_3$, 200 MHz): δ 2.27 (s + d, $^3J_{Pt,H}$ = 31.2 Hz, 3H, COCH$_3$), 2.52 (s + d, $^3J_{Pt,H}$ = 23.8 Hz, 3H, COCH$_3$), 7.20–7.32 (m, 5H, H^5 py + H^3 py + *p-H* Ph + *o-H* Ph), 7.43 (m, 2H, *m-H* Ph), 7.80 (m, 1H, H^4 py), 8.06 (s + d, $^3J_{Pt,H}$ = 24.4 Hz, 1H, CH=NNHPh), 8.36 (m, 1H, H^6 py), 11.63 (s + d, $^3J_{Pt,H}$ = 18 Hz, 1H, NH). ^{13}C NMR (CDCl$_3$, 100 MHz): δ 42.7 (s + d, $^2J_{Pt,C}$ = 375 Hz, COCH$_3$), 44.9 (s + d, $^2J_{Pt,C}$ = 347 Hz, COCH$_3$), 122.6–127.3 (4 × s, C^3 py + C^5 py + *p-C* Ph + *o-C* Ph), 129.9 (s, *m-C* Ph), 131.1 (s, CH=NNHPh), 137.9 (s, *i-C* Ph), 139.2 (s, C^4 py), 150.5 (s + d, $^2J_{Pt,C}$ = 43 Hz, C^6 py), 156.6 (s, C^2 py), 228.7 (s, COCH$_3$), 229.0 (s, COCH$_3$). ^{195}Pt NMR (CDCl$_3$, 86 MHz): δ −3395 (s). IR 2854(w), 1614(s), 1526(s) cm^{-1}.

[Pt(COMe)$_2$(2-pyCMe=NNHPh)] (**6b**). Yield: 58 mg (83%). Anal. found (calc.): C$_{17}$H$_{19}$N$_3$O$_2$Pt (492.44 g/mol): C 40.58 (41.46), H 3.79 (3.89), N 8.57 (8.53). ^{1}H NMR (CDCl$_3$, 200 MHz): δ 2.15 (s + d, $^3J_{Pt,H}$ = 29.7 Hz, 3H, COCH$_3$), 2.17 (s, 3H, C(CH$_3$)=NNHPh), 2.45 (s + d, $^3J_{Pt,H}$ = 23.3 Hz, 3H, COCH$_3$), 6.74 (m, 2H, *o-H* Ph), 6.96 (m, 1H, *p-H* Ph), 7.23 (m, 2H, *m-H* Ph), 7.52 (m, 1H, H^5 py), 7.70 (m, 1H, H^3 py), 8.02 (m, 1H, H^4 py), 8.61 (m, 1H, H^6 py), 10.65 (s + d, $^3J_{Pt,H}$ = 16 Hz, 1H, NH). ^{13}C NMR (CDCl$_3$, 100 MHz): δ 17.4 (s, C(CH$_3$)=NNHPh), 42.9 (s + d, $^2J_{Pt,C}$ = 371 Hz, COCH$_3$), 45.0 (s + d, $^2J_{Pt,C}$ = 342 Hz, COCH$_3$), 117.4 (s, *o-C* Ph), 122.9 (s, *p-C* Ph), 123.9 (s, C^3 py), 126.7 (s, C^5 py), 129.2 (s, *m-C* Ph), 139.4 (s, C^4 py), 144.1 (s, *i-C* Ph), 151.1 (s + d, $^2J_{Pt,C}$ = 42 Hz, C^6 py), 155.6 (s, C^2 py), 163.0 (s, C(CH$_3$)=NNHPh), 228.3 (s, COCH$_3$), 232.5 (s, COCH$_3$). ^{195}Pt NMR (CDCl$_3$, 86 MHz): δ −3404 (s). IR 2968(w), 2891(w), 1610(m), 1594(m), 1568(s), 1559(s), cm^{-1}.

[Pt(COMe)$_2$(2-pyCPh=NNHPh)] (**6c**). Yield: 56 mg (71%). HRMS (ESI): *m/z* calcd for [C$_{22}$H$_{21}$N$_3$O$_2$PtNa]$^+$ 577.11737, found for [M + Na]$^+$ 577.11731. ^{1}H NMR (CDCl$_3$, 400 MHz): δ 2.00 (s + d, $^3J_{Pt,H}$ = 27.9 Hz, 3H, COCH$_3$), 2.39 (s + d, $^3J_{Pt,H}$ = 23.5 Hz, 3H, COCH$_3$), 6.77 (m, 2H, *o-H* N–Ph), 6.84 (m, 1H, *p-H* N–Ph), 6.99 (m, 2H, *m-H* N–Ph), 7.06 (m, 1H, H^3 py), 7.10 (m, 2H, *o-H*/*m-H* C–Ph), 7.26 (m, 3H, *p-H* + *o*-H/*m-H* C–Ph), 7.38 (m, 1H, H^5 py), 7.74 (m, 1H, H^4 py), 8.62 (m, 1H, H^6 py), 9.97 (s + d, $^3J_{Pt,H}$ = 19 Hz, 1H, NH). ^{13}C NMR (CDCl$_3$, 100 MHz): δ 42.8 (s + d, $^2J_{Pt,C}$ = 367 Hz, COCH$_3$), 44.4 (s + d, $^2J_{Pt,C}$ = 361 Hz, COCH$_3$), 122.1 (s, *o-C* N–Ph), 124.7 (s, *p-C* N–Ph), 125.0 (s, C^3 py), 125.5 (s, C^5 py), 128.5 + 128.5 (2 × s, *m-C* N–Ph + *o-C*/*m-C* C–Ph), 129.1 (s, *o-C*/*m-C* C–Ph), 130.0 (s, *p-C* C–Ph), 131.5 (s, *i-C* C–Ph), 138.6 (s, C^4 py), 143.2 (s, *i-C* N–Ph), 150.8 (s + d, $^2J_{Pt,C}$ = 40 Hz, C^6 py), 155.4 (s, C^2 py), 156.4 (s, CPh=NNHPh), 228.7 (s + d, $^1J_{Pt,C}$ = 1294 Hz, COCH$_3$), 229.7 (s + d, $^1J_{Pt,C}$ = 1294 Hz, COCH$_3$). ^{195}Pt NMR (CDCl$_3$, 86 MHz): δ −3364 (s). IR 3155(w), 3049(w), 1634(w), 1591(s), 1528(m) cm^{-1}.

[Pt(COMe)$_2${2-pyCH=NNH(C$_6$F$_5$)}] (**6f**). Yield: 65 mg (79%). HRMS (ESI): *m/z* calcd for [C$_{16}$H$_{12}$F$_5$N$_3$O$_2$PtNa]$^+$ 591.03896, found for [M + Na]$^+$ 591.03847. ^{1}H NMR (CDCl$_3$, 200 MHz): δ 2.27 (s + d, $^3J_{Pt,H}$ = 32.8 Hz, 3H, COCH$_3$), 2.55 (s + d, $^3J_{Pt,H}$ = 23.3 Hz, 3H, COCH$_3$), 7.33–7.44 (m, 2H, H^5 + H^3 py), 7.60 (s + d, $^3J_{Pt,H}$ = 22 Hz, 1H, CH=NNH), 7.91 (m, 1H, H^4 py), 8.40 (m, 1H, H^6 py), 12.43 (s + d, $^3J_{Pt,H}$ = 18 Hz, 1H, NH). ^{13}C NMR (CDCl$_3$, 100 MHz): δ 42.3 (s + d, $^2J_{Pt,C}$ = 371 Hz, COCH$_3$), 44.7 (s + d, $^2J_{Pt,C}$ = 345 Hz, COCH$_3$), 123.9 + 125.1 (2 × s, C^3 py + C^5 py), 135.2 (s, CH=NNH), 136.9 (m, C_6F_5), 139.6 (s, C^4 py), 141.4 + 142.3 + 144.0 (3 × m, C_6F_5), 150.9 (s + d, $^2J_{Pt,C}$ = 42 Hz, C^6 py), 155.0 (s, C^2 py), 227.7 (s, COCH$_3$), 227.9 (s, COCH$_3$). ^{195}Pt NMR (CDCl$_3$, 86 MHz): δ −3415 (s). ^{19}F NMR (CDCl$_3$,

376 MHz): δ −159.90 (m, 2F, *m*-F), −153.14 (m, 1F, *p*-F), −142.13 (m, 2F, *o*-F). IR 2819(w), 1633(m), 1604(m), 1569(w) cm^{-1}.

*Syntheses of complexes **6d**/**c** with p-fluorophenylhydrazone ligands*

At room temperature, to a solution of [Pt(COMe)$_2$(NH$_2$Bn)$_2$] (**3**) (80 mg, 0.16 mmol) in methylene chloride (15 mL) 2-pyCR=NNH(C$_6$H$_4$-*p*-F) (R = H, Me) with an excess of 20% (0.19 mmol) was added. The reaction mixture was stirred for 24 h resulting in an orange colored suspension. After filtration, the volume of the solution was reduced to 1 mL and diethyl ether (3 mL) was added. The orange precipitate obtained was filtered off, washed with diethyl ether (3 × 3 mL), and dried in vacuo.

[Pt(COMe)$_2${2-pyCH=NNH(C$_6$H$_4$-*p*-F)}] (**6d**). Yield: 55 mg (69%). HRMS (ESI): *m/z* calcd for $[C_{16}H_{16}FN_3O_2PtNa]^+$ 519.07665, found for $[M + Na]^+$ 519.07685. ^{1}H NMR (CDCl$_3$, 500 MHz): δ 2.08 (s + d, $^3J_{Pt,H}$ = 33.5 Hz, 3H, COC*H*$_3$), 2.34 (s + d, $^3J_{Pt,H}$ = 23.7 Hz, 3H, COC*H*$_3$), 6.98 (m, 2H, *m*-*H* C$_6$*H*$_4$F), 7.04–7.09 (m, 4H, *H*^{5} py + *H*^{3} py + *o*-*H* C$_6$*H*$_4$F), 7.62 (m, 1H, *H*^{4} py), 7.69 (s + d, $^3J_{Pt,H}$ = 24 Hz, 1H, C*H*=NNH), 8.19 (m, 1H, *H*^{6} py), 11.37 (s + d, $^3J_{Pt,H}$ = 18 Hz, 1H, N*H*). ^{13}C NMR (CDCl$_3$, 125 MHz): δ 42.7 (s + d, $^2J_{Pt,C}$ = 370 Hz, COC*H*$_3$), 44.9 (s + d, $^2J_{Pt,C}$ = 347 Hz, COC*H*$_3$), 117.1 (d, $^2J_{F,C}$ = 22.7 Hz, *m*-*C* C$_6$H$_4$F), 122.7 + 123.9 (2 × s, *C*^{3} py + *C*^{5} py), 127.6 (d, $^3J_{F,C}$ = 8.6 Hz, *o*-*C* C$_6$H$_4$F), 131.5 (s, *C*H=NNH), 133.8 (d, $^4J_{F,C}$ = 3.2 Hz, *i*-*C* C$_6$H$_4$F), 139.3 (s, *C*^{4} py), 150.6 (s + d, $^2J_{Pt,C}$ = 38 Hz, *C*^{6} py), 156.4 (s, *C*^{2} py), 161.6 (d, $^1J_{F,C}$ = 248.6 Hz, *C*–F), 228.7 (s, *C*OCH$_3$), 229.1 (s, *C*OCH$_3$). ^{195}Pt NMR (CDCl$_3$, 86 MHz): δ −3397 (s). ^{19}F NMR (CDCl$_3$, 376 MHz): δ −112.71 (m). IR 3058(w), 2947(w), 1616(m), 1602(m), 1527(s) cm^{-1}.

[Pt(COMe)$_2${2-pyCMe=NNH(C$_6$H$_4$-*p*-F)}] (**6e**). Yield: 54 mg (65%). HRMS (ESI): *m/z* calcd for $[C_{17}H_{18}FN_3O_2PtNa]^+$ 533.09230, found for $[M + Na]^+$ 533.09254. ^{1}H NMR (CDCl$_3$, 200 MHz): δ 2.13 (s, 3H, C(*CH*$_3$)=NNH), 2.14 (s + d, $^3J_{Pt,H}$ = 29.6 Hz, 3H, COC*H*$_3$), 2.44 (s + d, $^3J_{Pt,H}$ = 23.3 Hz, 3H, COC*H*$_3$), 6.74 (m, 2H, *o*-*H* C$_6$*H*$_4$F), 6.93 (m, 2H, *m*-*H* C$_6$*H*$_4$F), 7.52 (m, 1H, *H*^{5} py), 7.68 (m, 1H, *H*^{3} py), 8.00 (m, 1H, *H*^{4} py), 8.60 (m, 1H, *H*^{6} py), 10.60 (s + d, $^3J_{Pt,H}$ = 17 Hz, 1H, N*H*). ^{13}C NMR (CDCl$_3$, 100 MHz): δ 17.2 (s, C(*C*H$_3$)=NNH), 42.8 (s + d, $^2J_{Pt,C}$ = 375 Hz, COCH$_3$), 45.0 (s + d, $^2J_{Pt,C}$ = 347 Hz, COCH$_3$), 115.9 (d, $^2J_{F,C}$ = 22.8 Hz, *m*-*C* C$_6$H$_4$F), 119.5 (d, $^3J_{F,C}$ = 8.0 Hz, *o*-*C* C$_6$H$_4$F), 123.9 (s, *C*^{3} py), 126.8 (s, *C*^{5} py), 139.4 (s, *C*^{4} py), 140.6 (d, $^4J_{F,C}$ = 2.7 Hz, *i*-*C* C$_6$H$_4$F), 151.1 (s + d, $^2J_{Pt,C}$ = 40 Hz, *C*^{6} py), 155.5 (s, *C*^{2} py), 158.8 (d, $^1J_{F,C}$ = 242.4 Hz, *C*–F), 162.8 (s, *C*(CH$_3$)=NNH), 228.3 (s, *C*OCH$_3$), 232.3 (s, *C*OCH$_3$). ^{195}Pt NMR (CDCl$_3$, 86 MHz): δ −3408 (s). ^{19}F NMR (CDCl$_3$, 376 MHz): δ −119.76 (m). IR 3076(w), 2949(w), 1617(s), 1597(m), 1559(s) cm^{-1}.

*Syntheses of complexes **7** bearing acyl substituted hydrazone ligands*

The procedure is analogous to that described for the syntheses of complexes **6a**–**c** (see above), but with a shortened reaction time of 6 h.

[Pt(COMe)$_2${2-pyCH=NNH(COMe)}] (**7a**). Yield: 52 mg (83%). HRMS (ESI): *m/z* calcd for $[C_{12}H_{16}N_3O_3Pt]^+$ 445.08339, found for $[M + H]^+$ 445.08339. ^{1}H NMR (CDCl$_3$, 200 MHz): δ 2.26 (s + d, $^3J_{Pt,H}$ = 32.5 Hz, 3H, Pt–COC*H*$_3$), 2.28 (s, 3H, N–COC*H*$_3$), 2.52 (s + d, $^3J_{Pt,H}$ = 23.4 Hz, 3H, Pt–COC*H*$_3$), 7.48 (m, 1H, *H*^{5} py), 7.64 (m, 1H, *H*^{3} py), 7.99 (m, 1H, *H*^{4} py), 8.48 (m, 1H, *H*^{6} py), 10.33 (s + d, $^3J_{Pt,H}$ = 26.0 Hz, 1H, C*H*=NNH), 13.50 (s + d, $^3J_{Pt,H}$ = 18 Hz, 1H, N*H*). ^{13}C NMR (CDCl$_3$, 100 MHz): δ 23.6 (s, N–COC*H*$_3$), 42.5 (s + d, $^2J_{Pt,C}$ = 374 Hz, Pt–COCH$_3$), 44.7 (s + d, $^2J_{Pt,C}$ = 340 Hz, Pt–COC*H*$_3$), 126.2 (s, *C*^{3} py), 126.7 (s, *C*^{5} py), 139.9 (s, *C*^{4} py), 150.4 (s, *C*H=NNH), 151.2 (s, *C*^{6} py), 155.6 (s, *C*^{2} py), 169.0 (s, N–*C*OCH$_3$), 227.9 (s, Pt–*C*OCH$_3$), 228.5 (s, Pt–*C*OCH$_3$). ^{195}Pt NMR (CDCl$_3$, 86 MHz): δ −3411 (s). IR 3053(w), 2960(w), 1682(w), 1621(m), 1552(w) cm^{-1}.

[Pt(COMe)$_2${2-pyCMe=NNH(COMe)}] (**7b**). Yield: 49 mg (76%). HRMS (ESI): *m/z* calcd for $[C_{13}H_{17}N_3O_3PtNa]^+$ 481.08099, found for $[M + Na]^+$ 481.08091. ^{1}H NMR (CDCl$_3$, 200 MHz): δ 2.22 (s, 3H, N–COC*H*$_3$); 2.23 (s + d, $^3J_{Pt,H}$ = 30.5 Hz, 3H, Pt–COC*H*$_3$), 2.27 (s, 3H, C(C*H*$_3$)=NNH), 2.45 (s + d, $^3J_{Pt,H}$ = 23.1 Hz, 3H, Pt–COC*H*$_3$), 7.54 (m, 1H, *H*^{5} py), 7.81 (m, 1H, *H*^{3} py), 8.04 (m, 1H, *H*^{4} py), 8.53 (m, 1H, *H*^{6} py), 12.40 (s + d, $^3J_{Pt,H}$ = 15 Hz, 1H, N*H*). ^{13}C NMR (CDCl$_3$, 100 MHz): δ 18.4 (s, C(*C*H$_3$)=NNH), 22.3 (s, N–*C*OCH$_3$), 42.7 (s + d, $^2J_{Pt,C}$ = 370 Hz, Pt–*C*OCH$_3$), 44.0 (s + d, $^2J_{Pt,C}$ = 339 Hz, Pt–*C*OCH$_3$), 125.2 (s, *C*^{3} py), 127.5 (s, *C*^{5} py), 139.6 (s, *C*^{4} py), 151.0 (s, *C*^{6} py), 155.2 (s, *C*^{2} py), 166.7 (s, *C*(CH$_3$)=NNH), 167.1 (s, N–*C*OCH$_3$), 228.7 (s, Pt–*C*OCH$_3$), 230.4 (s, Pt–*C*OCH$_3$). ^{195}Pt NMR (CDCl$_3$, 86 MHz): δ −3392 (s). IR 3132(w) 3047(w), 1716(m) 1618(m), 1596(w), 1560(m) cm^{-1}.

[Pt(COMe)$_2${2-pyCH=NNH(COPh)}] (**7c**). Yield: 56 mg (78%). Anal. found (Calc.): $C_{17}H_{17}N_3O_3Pt$ (506.42 g/mol), C 39.57 (40.32), H 3.11 (3.38), N 8.07 (8.30). ^{1}H NMR (CDCl$_3$, 400 MHz): δ 2.28 (s + d, $^3J_{Pt,H}$ = 32.4 Hz, 3H, COC*H*$_3$), 2.54 (s + d, $^3J_{Pt,H}$ = 23.5 Hz, 3H, COC*H*$_3$), 7.47 (m, 1H, *H*^{5} py), 7.55 (m, 3H, *m*-*H* + *p*-*H* Ph), 7.69 (m, 1H, *H*^{3} py), 8.00 (m, 1H, *H*^{4} py), 8.16 (m, 2H, *o*-*H* Ph), 8.48 (m, 1H, *H*^{6} py), 10.60 (s + d, $^3J_{Pt,H}$ = 26.2 Hz, 1H, C*H*=NNH), 14.25 (s + d, $^3J_{Pt,H}$ = 18 Hz, 1H, N*H*). ^{13}C NMR (CDCl$_3$, 100 MHz): δ 42.4 (s + d, $^2J_{Pt,C}$ = 370 Hz, COCH$_3$), 44.7 (s + d, $^2J_{Pt,C}$ = 346 Hz, COC*H*$_3$), 126.3 (s, *C*^{3} py), 126.7 (s, *C*^{5} py), 127.7 (s, *o*-*C* Ph), 129.1 (s, *m*-*C* Ph), 132.1 (s, *i*-*C* Ph), 132.9 (s, *p*-*C* Ph), 139.9 (s, *C*^{4} py), 150.8 (s, *C*H=NNH), 151.1 (s, *C*^{6} py), 155.7 (s, *C*^{2} py), 165.9 (s, *C*OPh), 227.7 (s, *C*OCH$_3$), 229.1 (s, *C*OCH$_3$). ^{195}Pt NMR (CDCl$_3$, 86 MHz): δ −3413 (s). IR 3057(w), 2966(w) 1674(w), 1615(m), 1579(w) cm^{-1}.

[Pt(COMe)$_2${2-pyCMe=NNH(COPh)}] (**7d**). Yield: 61 mg (83%). HRMS (ESI): *m/z* calcd for $[C_{18}H_{19}N_3O_3PtNa]^+$ 543.09664, found for $[M + Na]^+$ 543.09631. ^{1}H NMR (CDCl$_3$, 400 MHz): δ 2.21 (s + d, $^3J_{Pt,H}$ = 30.9 Hz, 3H, COC*H*$_3$), 2.35 (s, 3H, C(C*H*$_3$)=NNH), 2.48 (s + d, $^3J_{Pt,H}$ = 22.9 Hz, 3H, COC*H*$_3$), 7.50–7.60 (m, 4H, *H*^{5} py + *m*-*H* Ph + *p*-*H* Ph), 7.85 (m, 1H, *H*^{3} py), 8.06 (m, 1H, *H*^{4} py), 8.13 (m, 2H, *o*-*H* Ph), 8.58 (m, 1H, *H*^{6} py), 13.34 (s + d, $^3J_{Pt,H}$ = 17 Hz, 1H, N*H*). ^{13}C NMR (CDCl$_3$, 100 MHz): δ 18.7 (s, pyC(*C*H$_3$)=NNH(COPh)), 42.6 (s + d, $^2J_{Pt,C}$ = 370 Hz, COCH$_3$), 44.9 (s + d, $^2J_{Pt,C}$ = 340 Hz, COC*H*$_3$), 125.2 (s, *C*^{3} py), 127.5 (s, *C*^{5} py), 128.2 (s, *o*-*C* Ph), 129.0 (s, *m*-*C* Ph), 131.6 (s, *i*-*C* Ph), 132.8 (s, *p*-*C* Ph), 139.7 (s, *C*^{4} py), 151.1 (s + d, $^2J_{Pt,C}$ = 40 Hz, *C*^{6} py), 155.4 (s, *C*^{2} py), 163.2 (s, py*C*(CH$_3$)=NNH(COPh)), 166.9 (s, *C*OPh), 229.0 (s, *C*OCH$_3$), 230.4 (s, *C*OCH$_3$). ^{195}Pt NMR (CDCl$_3$, 86 MHz): δ −3396 (s). IR 3134(w), 3051(w), 1688(m), 1622(m), 1599(w), 1551(m) cm^{-1}.

[Pt(COMe)$_2${2-pyCH=NNH{CO(C$_6$H$_4$-*p*-F)}}] (**7e**). Yield: 63 mg (84%). HRMS (ESI): *m/z* calcd for $[C_{17}H_{17}FN_3O_3Pt]^+$ 525.08962, found for $[M + H]^+$ 525.09025. ^{1}H NMR (CDCl$_3$, 500 MHz): δ 2.33 (s + d, $^3J_{Pt,H}$ = 32.8 Hz, 3H, COC*H*$_3$), 2.59 (s + d, $^3J_{Pt,H}$ = 23.4 Hz, 3H, COC*H*$_3$), 7.27 (m, 2H, *m*-*H* C$_6$H$_4$F), 7.52 (m, 1H, *H*^{5} py), 7.75 (m, 1H, *H*^{3} py), 8.05 (m, 1H, *H*^{4} py), 8.25 (m, 2H, *o*-*H* C$_6$H$_4$F), 8.52 (m, 1H, *H*^{6} py), 10.60 (s + d, $^3J_{Pt,H}$ = 25.2 Hz, 1H, C*H*=NNH), 14.35 (s + d, $^3J_{Pt,H}$ = 20 Hz, 1H, N*H*). ^{13}C NMR (CDCl$_3$, 125 MHz): δ 42.4 (s + d, $^2J_{Pt,C}$ = 374 Hz, COCH$_3$), 44.7 (s + d, $^2J_{Pt,C}$ = 347 Hz, COCH$_3$), 116.3 (d, $^2J_{F,C}$ = 22.1 Hz, *m*-*C* C$_6$H$_4$F), 126.4 (s, *C*^{3} py), 126.8 (s, *C*^{5} py), 128.3 (d, $^4J_{F,C}$ = 3.0 Hz, *i*-*C* C$_6$H$_4$F), 130.3 (d, $^3J_{F,C}$ = 9.3 Hz, *o*-*C* C$_6$H$_4$F), 139.9 (s, *C*^{4} py), 150.9 (s, *C*H=NNH), 151.2 (s, *C*^{6} py), 155.6 (s, *C*^{2} py), 164.7 (s, *C*O(C$_6$H$_4$F)), 165.6 (d, $^1J_{F,C}$ = 254.6 Hz, *C*–F), 227.8 (s + d, $^1J_{Pt,C}$ = 1310 Hz, COCH$_3$), 229.4 (s + d, $^1J_{Pt,C}$ = 1340 Hz, COCH$_3$). ^{195}Pt NMR (CDCl$_3$, 86 MHz): δ −3412 (s). ^{19}F NMR (CDCl$_3$, 376 MHz): δ −105.39 (m). IR 3407(w), 1658(w), 1633(m), 1579(w), 1596(m), 1550(w) cm^{-1}.

[Pt(COMe)$_2${2-pyCMe=NNH{CO(C$_6$H$_4$-*p*-F)}}] (**7f**). Yield: 52 mg (68%). HRMS (ESI): *m/z* calcd for $[C_{18}H_{18}FN_3O_3PtNa]^+$ 561.08721, found for $[M + Na]^+$ 561.08702. ^{1}H NMR (CDCl$_3$, 500 MHz): δ 2.20 (s + d, $^3J_{Pt,H}$ = 31.5 Hz, 3H, COC*H*$_3$), 2.34 (s, 3H, C(C*H*$_3$)=NNH), 2.48 (s + d, $^3J_{Pt,H}$ = 28.5 Hz, 3H, COC*H*$_3$), 7.20 (m, 2H, *m*-*H* C$_6$H$_4$F), 7.57

(m, 1H, H^5 py), 7.85 (m, 1H, H^3 py), 8.07 (m, 1H, H^4 py), 8.15 (m, 2H, *o*-*H* C_6H_4F), 8.57 (m, 1H, H^6 py), 13.40 (s + d, $^3J_{Pt,H} = 16$ Hz, 1H, N*H*). ^{13}C NMR ($CDCl_3$, 125 MHz): δ 18.8 (s, C(*C*H_3)=NNH), 42.7 (s + d, $^2J_{Pt,C} = 372$ Hz, CO*C*H_3), 44.9 (s + d, $^2J_{Pt,C} = 335$ Hz, CO*C*H_3), 116.1 (d, $^2J_{F,C} = 22.0$ Hz, *m*-*C* C_6H_4F), 125.2 (s, C^3 py), 127.5 (s, C^5 py), 127.9 (d, $^4J_{F,C} = 3.1$ Hz, *i*-*C* C_6H_4F), 130.7 (d, $^3J_{F,C} = 9.3$ Hz, *o*-*C* C_6H_4F), 139.7 (s, C^4 py), 151.1 (s, C^6 py), 155.3 (s, C^2 py), 162.3 (s, *C*(CH$_3$)=NNH), 165.5 (d, $^1J_{F,C} = 253.9$ Hz, *C*–F), 167.0 (s, *C*O(C_6H_4F)), 229.2 (s, CO*C*H_3), 230.4 (s, CO*C*H_3). ^{195}Pt NMR ($CDCl_3$, 86 MHz): δ −3395 (s). ^{19}F NMR ($CDCl_3$, 376 MHz): δ −105.73 (s (br)). IR 3151(w), 3053(w), 1686 (m), 1625(m), 1601(m), 1549(m) cm^{-1}.

Investigations on the reactivity of diacetyl platinum(II) complexes with amines

A solution of complex **4a**–**c**, **6d**/**f**, and **7c** (0.05 mmol) in CH_2Cl_2 (2 mL) was reacted with benzylamine (0.50 mmol and 5 mmol) at room temperature. After 2 h stirring, the solvent of the solution was reduced to about 0.5 mL, diethyl ether/*n*-pentane (2 mL, 1:1) was added and the precipitate was filtered off. NMR spectroscopic analyses showed the existence of the starting complexes **4a**–**c**, **6d**/**f**, and **7c**. Furthermore, complex **7e** (10 mg, 0.02 mmol) was treated with $NH_2CH_2CH_2Ph$ (0.05 mmol) in CD_2Cl_2, but NMR spectroscopically no reaction was observed within 1 day. The reaction of complex **7e** (10 mg, 0.02 mmol) with NH_2Et (ca. 400 μL) showed some unidentified decomposition products, but no iminoacetyl platinum(II) complex was found. **7e** (0.05 mmol) and benzylamine (0.20 mmol) in CH_2Cl_2 in the presence of molecular sieve (4A) did not show any reactivity.

X-ray crystallography

Crystals of [Pt(COMe)$_2$(2-pyCR=NNHR′)] (R/R′ = Me/H), **4b**; Ph/H, **4c**; H/Ph, **6a**; H/COMe, **7a**; H/COPh, **7c**; H/CO(C_6H_4-*p*-F, **7e**) and [Pt(COMe)$_2$(H_2NN=CMe–CMe=NNH_2)] (**5**) suitable for single-crystal X-ray diffraction analyses were obtained from CH_2Cl_2 solutions layered with *n*-pentane (**4b**, **6a**, **7a**, **7c**·CH_2Cl_2) and diethyl ether/*n*-pentane (**4c**, **5**). Crystals of **7e** were obtained from a tetrahydrofuran/*n*-pentane solution. Data for X-ray diffraction analyses of single crystals were collected on a Stoe-IPDS (**7a**) or a Stoe-IPDS 2T diffractometer (**4b**, **4c**, **5**, **6a**, **7c**·CH_2Cl_2, **7e**) at 200 K using Mo Kα radiation (λ = 0.71073 Å, graphite monochromator). A summary of the crystallographic data, the data collection parameters, and the refinement parameters is given in Tables S1–S3. Absorption corrections were applied empirically with the PLATON program package [16] (T_{min}/T_{max} 0.11/0.45, **4b**; 0.01/0.04, **4c**; 0.12/0.30, **5**; 0.02/0.07, **7a**) and numerically with X-RED32 [17] (T_{min}/T_{max} 0.28/0.76, **7c**·CH_2Cl_2; 0.16/0.29, **7e**). The structures were solved with direct methods using SHELXS-97 [18] and refined using full-matrix least-squares routines against F^2 with SHELXL-97 [19]. All non-hydrogen atoms were refined with anisotropic displacement parameters and hydrogen atoms with isotropic ones. H atoms were placed in calculated positions according to the riding model except those of the N–H···O and N–H···N hydrogen bonds which were located in the electron density map.

Computational details

DFT calculations were carried out with the Gaussian 09 program package [20] using the hybrid functional B3LYP [21]. For the main group atoms the basis sets 6-311++G(d,p) were employed as implemented in the Gaussian program. The valence electrons of platinum were approximated by a split valence basis set, too; for their core orbitals an effective core potential with consideration of relativistic effects was used [22]. The appropriateness of the functional in combination with the basis sets and effective core potential used for reliable interpretation of structural and energetic aspects of related platinum complexes has been demonstrated [23]. Molecules **4b***, **5***, and **7b*** were fully optimized without any restrictions. The resulting geometries were characterized as equilibrium structures by analysis of the force constants of the normal vibrations.

Appendix A. Supplementary material

CCDC 958319, 958320, 958321, 958322, 958323, 958324, and 958325 contain the supplementary crystallographic data for this paper. These data can be obtained free of charge from The Cambridge Crystallographic Data Centre via www.ccdc.cam.ac.uk/data_request/cif.

Appendix B. Supplementary data

Supplementary data related to this article can be found at http://dx.doi.org/10.1016/j.jorganchem.2014.03.030.

References

[1] T. Kluge, M. Bette, T. Rüffer, C. Bruhn, C. Wagner, D. Ströhl, J. Schmidt, D. Steinborn, Organometallics 32 (2013) 7090.
[2] D. Steinborn, Dalton Trans. (2005) 2664.
[3] S. Schwieger, F.W. Heinemann, C. Wagner, R. Kluge, C. Damm, G. Israel, D. Steinborn, Organometallics 28 (2009) 2485.
[4] T. Kluge, M. Bette, C. Vetter, J. Schmidt, D. Steinborn, J. Organomet. Chem. 715 (2012) 93.
[5] (a) M. Bette, J. Schmidt, D. Steinborn, Eur. J. Inorg. Chem. (2013) 2395;
(b) M. Bette, T. Kluge, J. Schmidt, D. Steinborn, Organometallics 32 (2013) 2216;
(c) M. Bette, T. Rüffer, C. Bruhn, J. Schmidt, D. Steinborn, Organometallics 31 (2012) 3700;
(d) T. Kluge, C. Mendicute-Fierro, M. Bette, A. Rodríguez-Diéguez, M.A. Garralda, D. Steinborn, Eur. J. Inorg. Chem. (2013) 5418.
[6] Cambridge Structural Database (CSD), Cambridge University Chemical Laboratory, Cambridge, 2013.
[7] (a) J. Bernstein, R.E. Davis, L. Shimoni, N.-L. Chang, Angew. Chem. Int. Ed. Engl. 34 (1995) 1555;
(b) M.C. Etter, J.C. MacDonald, J. Bernstein, Acta Crystallogr. B46 (1990) 256.
[8] (a) G.A. Jeffrey, An Introduction to Hydrogen Bonding, Oxford University Press, Oxford, 1997;
(b) T. Steiner, Angew. Chem. Int. Ed. 41 (2002) 48.
[9] M. Werner, C. Bruhn, D. Steinborn, J. Organomet. Chem. 693 (2008) 2369.
[10] (a) L. Brammer, J.M. Charnock, P.L. Goggin, R.J. Goodfellow, A.G. Orpen, T.F. Koetzle, J. Chem. Soc. Dalton Trans. (1991) 1789;
(b) L.M. Epstein, E.S. Shubina, Coord. Chem. Rev. 231 (2002) 165;
(c) N.V. Belkova, E.S. Shubina, L.M. Epstein, Acc. Chem. Res. 38 (2005) 624.
[11] H.K. Hall, J. Am. Chem. Soc. 79 (1957) 5441.
[12] (a) M.F. Mahon, J. McGinley, A.D. Rooney, J.M.D. Walsh, Tetrahedron 64 (2008) 11058;
(b) J.H. Boyer, R. Borgers, L.T. Wolford, J. Am. Chem. Soc. 79 (1957) 678.
[13] (a) R.P. Thummel, V. Hegde, J. Org. Chem. 54 (1989) 1720;
(b) A. Fernández, D. Vázquez-García, J.J. Fernández, M. López-Torres, A. Suárez, J.M. Vila, J. Organomet. Chem. 690 (2005) 3669;
(c) Q. Liu, M.S. Mudadu, H. Schmider, R. Thummel, Y. Tao, S. Wang, Organometallics 21 (2002) 4743.
[14] (a) P. Pelagatti, M. Carcelli, F. Franchi, C. Pelizzi, A. Bacchi, A. Fochi, H.-W. Frühauf, K. Goubitz, K. Vrieze, Eur. J. Inorg. Chem. (2000) 463;
(b) G. Palla, G. Predieri, P. Domiano, C. Vignali, W. Turner, Tetrahedron 42 (1986) 3649.
[15] D.H. Busch, J.C. Bailar Jr., J. Am. Chem. Soc. 78 (1956) 1137.
[16] (a) MULscanABS, PLATON for Windows Taskbar v1.15, University of Glasgow, 2008 (b) A.L. Spek, J. Appl. Crystallogr. 36 (2003) 7.
[17] X-RED32 (Version 1.07): Stoe Data Reduction Program, Stoe & Cie GmbH, Darmstadt, 2002.
[18] G.M. Sheldrick, SHEL XS-97, Program for Crystal Structure Solution, University of Göttingen, Göttingen, 1998.
[19] G.M. Sheldrick, SHEL XS-97, Program for the Refinement of Crystal Structures, University of Göttingen, Göttingen, 1997.
[20] M.J. Frisch, G.W. Trucks, H.B. Schlegel, G.E. Scuseria, M.A. Robb, J.R. Cheeseman, G. Scalmani, V. Barone, B. Mennucci, G.A. Petersson, H. Nakatsuji, M. Caricato, X. Li, H.P. Hratchian, A.F. Izmaylov, J. Bloino, G. Zheng, J.L. Sonnenberg, M. Hada, M. Ehara, K. Toyota, R. Fukuda,

J. Hasegawa, M. Ishida, T. Nakajima, Y. Honda, O. Kitao, H. Nakai, T. Vreven, J.A. Montgomery Jr., J.E. Peralta, F. Ogliaro, M. Bearpark, J.J. Heyd, E. Brothers, K.N. Kudin, V.N. Staroverov, T. Keith, R. Kobayashi, J. Normand, K. Raghavachari, A. Rendell, J.C. Burant, S.S. Iyengar, J. Tomasi, M. Cossi, N. Rega, J.M. Millam, M. Klene, J.E. Knox, J.B. Cross, V. Bakken, C. Adamo, J. Jaramillo, R. Gomperts, R.E. Stratmann, O. Yazyev, A.J. Austin, R. Cammi, C. Pomelli, J.W. Ochterski, R.L. Martin, K. Morokuma, V.G. Zakrzewski, G.A. Voth, P. Salvador, J.J. Dannenberg, S. Dapprich, A.D. Daniels, O. Farkas, J.B. Foresman, J.V. Ortiz, J. Cioslowski, D.J. Fox, Gaussian 09, Revision B.01, Gaussian, Inc., Wallingford CT, 2010.

[21] A.D. Becke, J. Chem. Phys. 98 (1993) 5648.

[22] (a) D. Andrae, U. Häußermann, M. Dolg, H. Stoll, H. Preuss, Theor. Chim. Acta 77 (1990) 123;
(b) See http://bse.pnl.gov/bse/portal.

[23] (a) K. Nordhoff, D. Steinborn, Organometallics 20 (2001) 1408;
(b) T. Gosavi, C. Wagner, H. Schmidt, D. Steinborn, J. Organomet. Chem. 690 (2005) 3229;
(c) M. Werner, T. Lis, C. Bruhn, R. Lindner, D. Steinborn, Organometallics 25 (2006) 5946;
(e) C. Vetter, C. Wagner, G.N. Kaluderovic, R. Paschke, D. Steinborn, Inorg. Chim. Acta 362 (2009) 189.